Original Article

Raman Spectroscopic Characterization of Hepatic Differentiation of Mesenchymal Stem Cells

Sareh Arjmand[1] **Ph.D., Aram Barzegar**[2] **M.Sc., Alemeh Mohammadpour**[3] **M.Sc., Hanieh Rezaei**[2] **M.Sc., Nahid Davoodian**[4] **Ph.D., Hori Ghaneialvar**[5,6] **Ph.D., Rasoul Malekfar**[2] **Ph.D., Abbas Sahebghadam Lotfi**[3*] **Ph.D.**

[1] Protein Research Center, Shahid Beheshti University, Tehran, Iran
[2] Department of Physics, Faculty of Basic Sciences, Tarbiat Modares University, Tehran, Iran
[3] Department of Clinical Biochemistry, Faculty of Medical Sciences, Tarbiat Modares University, Tehran, Iran
[4] Endocrinology and Metabolism Research Center, Hormozgan University of Medical Sciences, Bandar Abbas, Iran
[5] Department of Clinical Biochemistry, Faculty of Medicine, Ilam University of Medical Sciences, Ilam, Iran
[6] Biotechnology and Medicinal Plants Research Center, Ilam University of Medical Sciences, Ilam, Iran

A B S T R A C T

Background and Aims: Mesenchymal stem cells (MSCs) are a preferred cell source for the generation of hepatocyte-like cells in regenerative medicine. They can be isolated from different sources, including adipose tissues. The Raman spectroscopy approach was evaluated for quick and efficient identification of MSCs differentiation status and a broader perspective on cell differentiation.
Materials and Methods: The human adipose-derived mesenchymal stem cells (hASCs) were differentiated toward hepatocyte-like cells using a well-established method. The cells were cultured on fluorescence-free quartz discs, and the efficiency of differentiation was examined using molecular and biochemical methods. The Raman spectra were recorded at days 1, 7, 14, and 21 of differentiation, and HepG2 was used as a positive control.
Results: The changes in Raman spectra were detected during the sequential stages of differentiation, and the pattern of peaks on the last day of differentiation was remarkably similar to the positive control (HepG2).
Conclusion: Raman spectroscopy showed considerable potential to characterize hepatic differentiation.

*Corresponding Author: Department of Clinical Biochemistry, Faculty of Medical Sciences, Tarbiat Modares University, Tehran, Iran. Email: lotfi_ab@modares.ac.ir

Introduction

In many tissues, adult stem cells are responsible for homeostatic tissue maintenance and regenerative responses, owing to their self-renewal capacity and differentiation to more mature cells. Adult stem cells can be classified based on the origin and potential of differentiation. Mesenchymal stem cells (MSCs) are adult stem cells isolated from different sources, including bone marrow, umbilical cord, amniotic fluid, peripheral blood, and adipose tissue. These cells have a multipotent capacity for differentiation into different mesodermal lineages, such as osteoblasts, chondrocytes, and adipocytes [1]. The promising features of MSCs, including abundance, being easily accessed, remarkable genomic stability, low immunogenicity, and lack of ethical issues, make them the most commonly used cell sources for clinical applications such as cell therapy and regenerative medicine [2].

Directing and controlling the lineage/tissue-specific differentiation *in vitro* is one of the main challenges that should be overcome when differentiated stem cells are needed for cell or tissue therapy. Numerous studies have been conducted, which used different strategies, such as using different induction conditions and platforms or scaffolds for different purposes, from cell therapy to tissue engineering [3, 4]. A substantial number of clinical trials are currently underway to investigate the application of MSCs in the treatment of various health disorders [5, 6]. Since it is impossible to simulate the identical dynamic *in vivo* microenvironment, differentiated cells with 100% similarity to the target cell have not been constructed so far. However, cells with different degrees of resemblance have been obtained that have high clinical and research values [7].

A key point in all of the cited studies is to evaluate the degree of similarity between the differentiated cells and target cells, which will be replaced with, and a comparison of the differentiation process in different methods at molecular levels. The obtained cells are generally characterized by various molecular, immunological, and biochemical methods, including morphological analysis and quantitative or qualitative measurement of tissue-specific genes expression, metabolite, and other biomarkers inside the cells or in the microenvironment. Due to the time and cost constraints, a limited number of cell criteria are commonly characterized to evaluate each study's differentiation [8]. A variety of methods have been developed for tracing the stem cells during proliferation and differentiation. These analyzing methods help us optimize their isolation and regulation techniques for therapeutic applications [9, 10]. Developing a cost/time-effective and reproducible method for cell status characterization will better understand the stem cell differentiation process, and Raman spectroscopy can be considered a potential candidate. Raman spectroscopy is an analytical technique, without using any dye or label, which has been employed in different aspects of biological research in recent decades. In cell biology, this spectroscopy resulted in the spectral band markers obtained through the

inelastic scattering of laser light and are ascertained as a differentiator of different cells and tissues [11]. According to previous studies, the Raman technique's data have fingerprinting characteristics and covers the overall cellular constitution, including nucleic acids, proteins, lipids, carbohydrates, and minerals [12]. Here, the Raman spectroscopic cell imaging approach was proposed to identify sequential stem cell differentiation rapidly.

Materials and Methods

Human adipose-derived mesenchymal stem cells (hASCs) isolation and characterization

To isolate hASCs, after signing informed consent and approval by the Ethics Committee of Tarbiat Modares University (IR.TMU.REC.1396.672), lipoaspirate was obtained from the subcutaneous fat of a healthy 40-years-old woman donor who has undergone abdominal liposuction during cosmetic surgery. Isolation of hASCs was performed as described earlier [13]. Briefly, lipoaspirate was treated with 0.075% collagenase I (Sigma-Aldrich) at 37 ℃ for 30 min. After centrifugation, the extracted cells were suspended in Dulbecco's modified Eagle's medium (DMEM) (Gibco) supplemented with 10% fetal bovine serum (Gibco) and 1% penicillin/ streptomycin (Sigma-Aldrich) and finally incubated in a humidified atmosphere at 37 ℃ containing 5% CO2. Non-adherent cells were removed after two days and washed away when the medium was changed. The purified attached stem cells were obtained after three days. After reaching 70-80% of confluency, the cells were harvested (passage 0) and stored in liquid nitrogen at -180°C for the following application.

Cell surface antigen analysis

For flow cytometric analysis, first passage cells were detached and labeled with PE-conjugated mouse anti-human CD34, CD44, CD105, and FITC-conjugated mouse anti-human CD45 and CD90 (Abcam, USA). Then, the labeled cells were evaluated using a BD FACSCalibur cytometer (Becton Dickinson, USA).

Hepatic differentiation of hASCs

Fluorescence-free quartz discs, suitable for Raman spectroscopy, were prepared with a 15 mm diameter × 0.5 mm thickness dimension. Heat-sterilized quartz discs were fitted at the bottom of 4-well plates. At passage three, 1×10^3 hASCc were plated at quartz discs, and hepatic differentiation was performed according to a two-step protocol described earlier [14]. Briefly, the cells were treated with DMEM supplemented with 10% fetal bovine serum, 20 ng/ml hepatocyte growth factor, and 10^{-7} mol/l dexamethasone for a week, followed by the addition of oncostatin M (OSM, 10 ng/ml) to the medium for the next two weeks. The culture medium was refreshed twice a week, and the finally obtained hepatocyte-like cells were characterized using biochemical and molecular experiments.

Quantitative real-time polymerase chain reaction (qPCR) analysis

For qPCR analysis, total RNA was extracted using Tryzol reagent (Sigma-Aldrich) on days 1, 7, 14, and 21 of differentiation according to the previously described protocol [15]. The extracted RNA was reverse transcribed to complementary DNA (cDNA) using AccuPower® CycleScript RT PreMix (K-2046, Bioneer) per the manufacturer's instructions.

The expression of four hepatocyte-specific genes (*albumin* (*ALB*), *α-fetoprotein* (*AFP*), and *cytokeratin 18* and *19* (*CK18* and *19*) were analyzed using qPCR according to the previously reported procedure [15]. Shortly, a three-step procedure was used: denaturation at 95 °C for 30 s, annealing at 60 °C for 30 s, and extension at 72°C for 60 s (40 cycles). β-actin was used as an internal control, and all qPCR reactions were done in triplicate. Finally, the $2^{-\Delta\Delta Ct}$ method was used to calculate the relative quantification of gene expression. The list of primers is shown in Table 1.

Glycogen storage and urea production

Glycogen storage was determined by Periodic Acid Schiff's (PAS) staining in hepatocyte-like cells at day 21 of differentiation. To this end, the cells were fixed in 4% paraformaldehyde, oxidized in 1% periodic acid for 5 min, treated with Schiff's reagent (Sigma, 395-2-016) for 15 min, and stained with Mayer's hematoxylin for 1 min. Finally, the stained cells were visualized with an inverted microscope.

According to the manufacturer's recommendation and analyzed using a photometer, urea concentration in cells' culture media was determined by colorimetric assay (URA-S, ZiestChemie Diagnostics). The supernatant of hASCs and HepG2 cell culture was used as the negative and positive controls, respectively. Urea concentrations were normalized to the number of cells in each well.

Backscattering for Raman spectroscopy

Raman spectroscopy was employed immediately on the cells attached to the quartz surface after decanting the supernatant liquid. The spectra were collected at room temperature using a Thermo Nicolet Almega Dispersive Raman spectrometer (USA) equipped with a second harmonic 532 nm laser line in a backscattering configuration. The slit width was set to 20 micrometers and a Raman spectrum resolution of about 4 cm^{-1}. The detection system was a low-temperature CCD detector operating at -65ºC. The experiment was repeated three times, and the mean values were used for the analysis. The quartz background spectrum was subtracted from that of the samples, and the spectral maps were analyzed using the Omnic 6.0 software (Thermo Nicolet Co., USA).

Statistical analysis

The data were expressed as mean ± standard deviation (SD). One-way analysis of variance (ANOVA) was performed for analysis followed by LSD post hoc test using SPSS version 23 software. The p-value of < 0.05 was considered statistically significant.

Table 1. The sequence of using primers for qPCR

Gene	Primers
ALB	F: 5'-GAGACCAGAGGTTGATGTGATG-3' R: 5'-AGGCAGGCAGCTTTATCAGCA-3'
AFP	F: 5'-TTGATGACACCAATATCACACGA-3' R: 5'-TATTGGGCCCGGATGTCTG-3'
CK18	F: 5'-TTGATGACACCAATATCACACGA-3' R: 5'-TATTGGGCCCGGATGTCTG-3'
CK19	F: 5'-CGAACCAAGTTTGAGACGGAAC-3' R: 5'-CGTACTGATTTCCTCCTCATGG-3'
β-actin	F: 5'-CTGGAACGGTGAAGGTGACA-3' R: 5'- AAGGGACTTCCTGTAACAATGCA-3'

Results

Characterization of hASCs

The results revealed the high positive expression of MSCs surface markers: CD44 (98%), CD105 (98%), CD90 (98%) and low expression of hematopoietic surface markers: CD34 (2%) and CD45 (2%).

Hepatic differentiation and characterization

As illustrated in Figure 1A, the morphological changes of cells were evaluated at various hepatic differentiation protocol stages. However, no significant morphological alterations were observed during the first week of differentiation induction; the cells started to lose fibroblastic morphology and flattened on day 14. Interestingly, after 21 days, most of the cells displayed hepatocytes' characteristics, including a polygonal shape and cytoplasmic granulation. As illustrated in Figure 1B, AFP was significantly expressed at day 14 (4-fold, $p < 0.01$) and further increased at day 21 (10-fold, $p < 0.001$) in hepatocyte-like cells. Consistently, a similar expression pattern was observed for ALB with a significant upregulation at day 14 to 4.5 fold ($p < 0.05$) that reach a maximum level of 7.5 fold ($p < 0.01$) on day 21 compared to day 1 of hepatic differentiation induction. No differences in CK19 expression levels were noticed at different differentiation protocol stages; a significant upregulation in CK18 expression was detected at day 21 to nearly 2.5 fold ($p < 0.05$). These results were further confirmed with functional assays of hepatocyte-like cells. PAS staining experiment indicated the differentiated cells' ability for glycogen storage (Fig. 2A),

which is the characteristic of hepatocyte cells. The differentiated cells also showed a significantly higher ability to produce urea ($p < 0.01$) compared to the primary hASCs as the negative control (Fig. 2B).

Raman spectroscopy analysis

In the first step, the Raman spectra of HepG2 and MSCs were recorded, and the results indicated that Raman spectroscopy could provide a different, specific, and reproducible spectrum for the two cell types in a few minutes. Figure 3A illustrates the recorded vibrational modes of the two cell types. The spectral bands' differences are related to the difference in cells' chemical structures [16]. During the differentiation process toward hepatocyte-like cells, the Raman spectra of cells were recorded every seven days and compared to the undifferentiated (hASCs) and fully differentiated (HepG2) cells as the negative and positive controls. For ease of comparison and interpretation of the results, the plots were overlaid (Fig. 3B). The band at 801 cm^{-1} (region A) shows the O-P-O bonding in RNA and confirms proteins' presence. The Raman modes at 1345 cm^{-1} (region B) are due to DNA and RNA and confirm lipids and phospholipids' presence. Regions C and D are near the vibration of $C = O$ and C-N molecules, respectively. The vibrational band at 2415 cm^{-1} (region E) is assigned to CO_2, and the modes at around 2134 cm^{-1} are due to the C-N bond. The CH_2 groups vibrate at region F (2751 cm^{-1}). The Raman band at 2953 cm^{-1} (region G) is due to asymmetric vibrations of CH_3, and the peak in this spectral region shows the presence of lipids

and fatty acids. The band at 3264 cm^{-1} is assigned to the N-H group. The OH stretching vibration located at 3500 cm^{-1} is assigned to H$_2$O molecules [17-19].
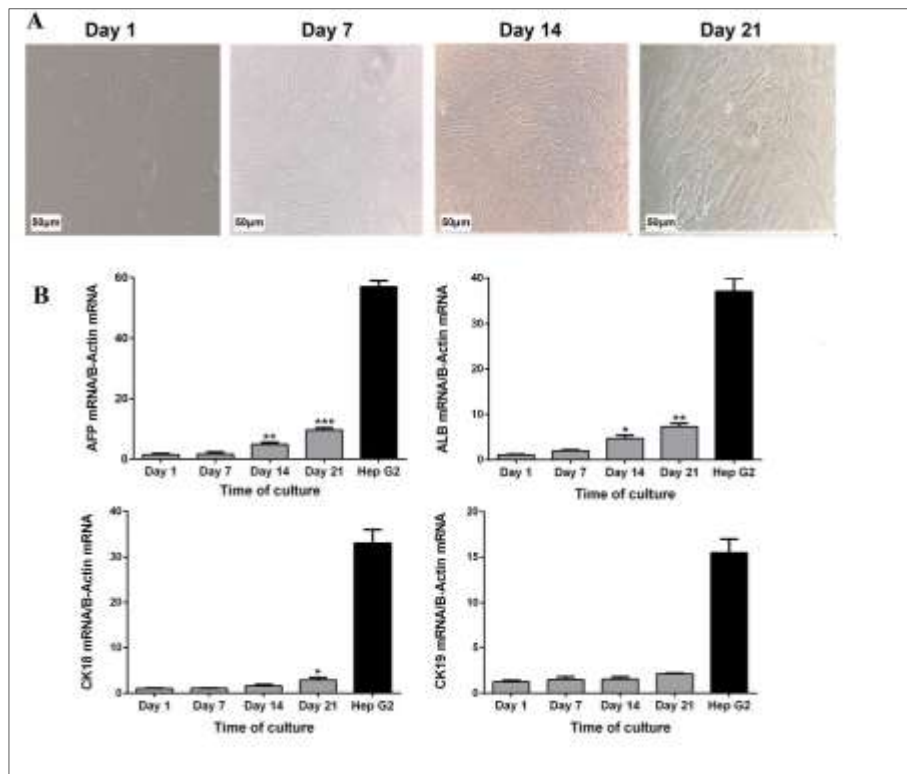

Fig. 1. A) Morphological changes of human adipose-derived mesenchymal stem cells during hepatic differentiation induction. B) Quantitative analysis of hepatic expression genes in days 7, 14, and 21 of differentiation. The expression of the same genes in HepG2 was used as a positive control. *β-actin* expression was used as a reference gene. The data are shown as mean±SEM in three independent experiments (n=3). *p <0.05, **p <0.01, ***p <0.001 relative to day1.
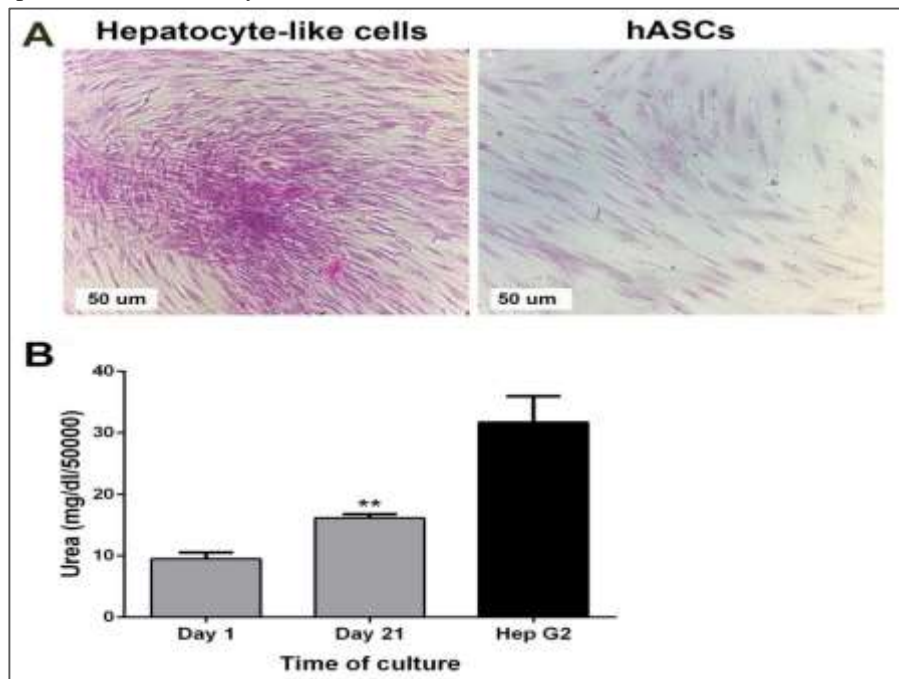

Fig. 2. A) Periodic acid schiff's staining of differentiated hepatocyte-like cells compared to undifferentiated stem cells as the negative controls. B) The ureagenesis was improved in differentiated hepatocyte like-cells. The data are expressed as mean±SEM (n=3). **p <0.01 relative to day 1.
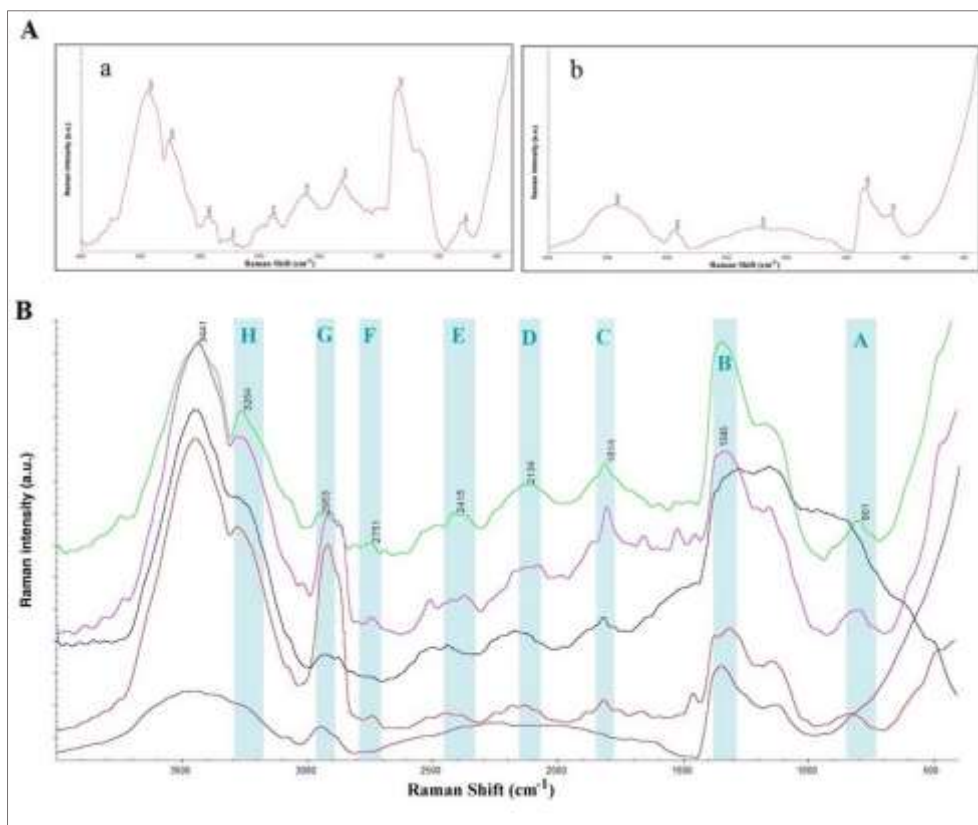
Fig. 3. A) Raman spectra of a) HepG2, and b) Human adipose-derived mesenchymal stem cells. B) The overlaid plots of Raman spectra, recorded at different days of differentiation. Human adipose-derived mesenchymal stem cells and HepG2 were used as negative and positive controls, respectively (n=3).

Discussion

Raman spectroscopy has an excellent specificity for characterizing biological samples' molecular phenotype and quantifying the molecular changes at the cellular level [20]. Lots of studies used this spectroscopic technique for cellular studies. It has been used to discriminate between normal, malignant, and metastatic cells [21]. It is deduced from the results that the content of RNA, DNA, lipids, and proteins was gradually raised during the differentiation process, and the pattern of peaks at the last day of differentiation was remarkably similar to the control (HepG2), eventhough it is not completely identical. This result aligns with the molecular and biochemical results indicating a relative similarity between differentiated and control cells. Furthermore, HepG2 is a cell line and expected to be different from normal hepatocytes [22]. However, it is accepted as an appropriate model for *in vitro* studies [23, 24]. A variety of studies used different methods for enhancing differentiation efficiency, including hepatocyte differentiation [15]. The efficiency of methods was generally evaluated using different molecular and biochemical methods. New non-invasive, real-time methods for tracking stem cell status and degree of differentiation can significantly improve our understanding of stem cells' behavior and control their fate. Here, Raman spectroscopy was introduced as a new potent method that can be

studied, quantified, and optimized for rapid and label-free evaluation of human hASCs during and at the end of the differentiation procedure toward hepatocytes. The results indicated that the obtained spectra are particular and unique. The observed differences are related to the difference in the chemical structures of cells [16] and can be used to detect differentiation quality in a few minutes. So far, this method has been used to study biochemical changes commensurate with the osteogenic, cardiogenic, neurogenic, and adipogenic differentiation of stem cells [25, 26]. Furthermore, Raman spectroscopy was introduced as a biosensor for molecular characterization of mouse-derived MSCs during differentiation to hepatocytes [27].

Conclusion

Overall, it is suggested that this method has considerable potential in various cell studies, including identifying the cell types and their differentiation stage and analyzing the techniques used in improving stem cell differentiation. Raman spectroscopy can complement conventional molecular and biochemical techniques of cell studies and overcome some of their limitations, such as time and cost.

Conflict of Interest
The authors declare no conflict of interest.

Acknowledgment
Not applicable.

References

[1]. Ullah I, Subbarao RB, Rho GJ. Human mesenchymal stem cells - current trends and future prospective. Biosci Rep. 2015; 35(2): 191.

[2]. Horwitz EM, Le Blanc K, Dominici M, Mueller I, Slaper-Cortenbach I, Marini FC, et al. Clarification of the nomenclature for MSC: The International Society for Cellular Therapy position statement. Cytotherapy 2005; 7(5): 393-395.

[3]. Davoodian N, Lotfi AS, Soleimani M, Mola SJ, Arjmand S. Let-7f microRNA negatively regulates hepatic differentiation of human adipose tissue-derived stem cells. J Physiol Biochem. 2014; 70(3): 781-789.

[4]. Mohammadpour A, Arjmand S, Lotfi AS, Tavana H, Kabir-Salmani M. Promoting hepatogenic differentiation of human mesenchymal stem cells using a novel laminin-containing gelatin cryogel scaffold. Biochem Biophys Res Commun. 2018; 507(1-4): 15-21.

[5]. Golchin A, Farahany TZ, Khojasteh A, Soleimanifar F, Ardeshirylajimi A. The clinical trials of mesenchymal stem cell therapy in skin diseases: an update and concise review. Curr Stem Cell Res Ther. 2019; 14(1): 22-33.

[6]. Kusakawa S, Sawada R, Yasuda S, Kuroda T, Sato Y. Trends in global clinical trial registration for MSC-based therapeutic products. Cytotherapy 2020; 22(5): S165.

[7]. Chen FM, Liu X. Advancing biomaterials of human origin for tissue engineering. Prog Polym Sci. 2016; 53: 86-168.

[8]. Moura CC, Tare RS, Oreffo RO, Mahajan S. Raman spectroscopy and coherent anti-Stokes Raman scattering imaging: prospective tools for monitoring skeletal cells and skeletal regeneration. J R Soc Interface 2016; 13(118): 1-12.

[9]. Alexander MS, Casar JC, Motohashi N. Stem cell differentiation and therapeutic use. Stem Cells Int. 2015; 2015: 308128.

[10]. Cen P, Chen J, Hu C, Fan L, Wang J, Li L. Noninvasive in-vivo tracing and imaging of transplanted stem cells for liver regeneration. Stem Cell Res Ther. 2016; 7(1): 143.

[11]. Ember KJI, Hoeve MA, McAughtrie SL, Bergholt MS, Dwyer BJ, Stevens MM, et al. Raman spectroscopy and regenerative medicine: a review. NPJ Regen Med. 2017; 2(12): 1-10.

[12]. Brauchle E, Schenke-Layland K. Raman spectroscopy in biomedicine - non-invasive in vitro analysis of cells and extracellular matrix components in tissues. Biotechnol J. 2013; 8(3): 288-297.

[13]. Zuk PA, Zhu M, Mizuno H, Huang J, Futrell JW, Katz AJ, et al. Multilineage cells from human adipose tissue: implications for cell-based therapies. Tissue Eng. 2001; 7(2): 211-228.

[14]. Khalaj Z, Lotfi AS, Kabir-Salmani M. Laminin matrix promotes hepatogenic terminal differentiation of human bone marrow mesenchymal stem cells. Iran J Basic Med Sci. 2016; 19(1): 34-42.

[15]. Mohammadpour A, Arjmand S, Lotfi AS, Tavana H, Kabir-Salmani M. Promoting hepatogenic differentiation of human mesenchymal stem cells using a novel laminin-containing gelatin cryogel scaffold. Biochem Biophys Res Commun. 2018; 507(1-4): 15-21.

[16]. Smith R, Wright KL, Ashton L. Raman spectroscopy: an evolving technique for live cell studies. Analyst 2016; 141(12): 3590-600.

[17]. Chen Y, Dai J, Zhou X, Liu Y, Zhang W, Peng G. Raman spectroscopy analysis of the biochemical characteristics of molecules associated with the malignant transformation of gastric mucosa. PLoS One 2014; 9(4): 93906.

[18]. Delfino I, Ricciardi V, Manti L, Lasalvia M, Lepore M. Multivariate analysis of difference raman spectra of the irradiated nucleus and cytoplasm region of SH-SY5Y human neuroblastoma cells. Sensors 2019; 19(18): 3971.

[19]. Guan Y, Wurrey CJ, Thomas Jr GJ. Vibrational analysis of nucleic acids. I. The phosphodiester group in dimethyl phosphate model compounds: (CH3O) 2PO2-,(CD3O) 2PO2-, and (13CH3O) 2PO2. Biophys J. 1994; 66(1): 225-235.

[20]. Corsetti S, Rabl T, McGloin D, Nabi G. Raman spectroscopy for accurately characterizing biomolecular changes in androgen-independent prostate cancer cells. J Biophotonics 2018; 11(3): 1700166.

[21]. Winnard P T, Zhang C, Vesuna F, Kang JW, Garry J, Dasari RR, et al. Organ-specific isogenic metastatic breast cancer cell lines exhibit distinct Raman spectral signatures and metabolomes. Oncotarget 2017; 8(12): 20266-20287.

[22]. Wiśniewski JR, Vildhede A, Norén A, Artursson P. In-depth quantitative analysis and comparison of the human hepatocyte and hepatoma cell line HepG2 proteomes. J Proteom 2016; 136: 234-247.

[23]. Aritomi K, Ishitsuka Y, Tomishima Y, Shimizu D, Abe N, Shuto T, et al. Evaluation of three-dimensional cultured HepG2 cells in a nano culture plate system: an in vitro human model of acetaminophen hepatotoxicity. J Pharmacol Sci. 2014; 124(2): 218-29.

[24]. Choi JM, Oh SJ, Lee SY, Im JH, Oh JM, Ryu CS, et al. HepG2 cells as an in vitro model for evaluation of cytochrome P450 induction by xenobiotics. Arch Pharm Res. 2015; 38(5): 691-704.

[25]. Mitchell A, Ashton L, Yang XB, Goodacre R, Smith A, Kirkham J. Detection of early stage changes associated with adipogenesis using Raman spectroscopy under aseptic conditions. Cytometry A 2015; 87(11): 1012-1019.

[26]. Su X, Fang S, Zhang D, Zhang Q, He Y, Lu X, et al. Quantitative Raman spectral changes of the differentiation of mesenchymal stem cells into islet-like cells by biochemical component analysis and multiple peak fitting. J Biomed Opt. 2015; 20(12): 125002.

[27]. Wu HH, Ho JH, Lee OK. Detection of hepatic maturation by Raman spectroscopy in mesenchymal stromal cells undergoing hepatic differentiation. Stem Cell Res Ther. 2016; 7(1): 6.